**4.3** STUDY OF DRAG COEFFICIENT AS A FUNCTION OF ATMOSPHERIC TURBULENCE AND OCEAN WAVE STATE

Tamara K. Grimmett, Gennaro H. Crescenti, and Timothy L. Crawford
Air Resources Laboratory Field Research Division
National Oceanic and Atmospheric Administration
Idaho Falls, Idaho

Douglas C. Vandemark
Laboratory for Hydrospheric Processes
NASA / Goddard Space Flight Center
Wallops Island, Virginia

## 1. INTRODUCTION

Existing parameterizations of heat, moisture, and momentum fluxes in the marine atmospheric boundary layer (MABL) perform poorly under weak wind regimes, especially in regions of inhomogeneity (e.g., Ramage 1984; Mahrt et al. 1996; Sun et al. 1996; Serra et al. 1997; Drennan et al. 1999; Greischar and Stull 1999; Lambert and Durand 1999). These problems are due to a variety of processes including averaging techniques, gravity/capillary wave spacing, surfactants and surface tension, free convection effects, and frequency-dependent differences between wind, waves, and stress. In order to improve our understanding of air-sea interaction in extremely light wind regimes, the Office of Naval Research (ONR) created the Coupled Boundary Layers Air-Sea Transfer (CBLAST) Defense Research Initiative (DRI). The objectives of the CBLAST light-wind initiative are (1) to measure vertical fluxes of momentum and heat in the lower atmospheric boundary layer and in the ocean surface layer; (2) to identify the processes that influence these fluxes (e.g., shear, convection, surface wave breaking, Langmuir cells); (3) to close budgets for heat and momentum; (4) to test parameterizations of fluxes; and (5) to obtain other measurements (e.g., horizontal variability of pressure and temperature) sufficient to provide boundary conditions for a large eddy simulation or local application of a regional-scale simulation.

A small research aircraft was used in the CBLAST-Low pilot field study to acquire high-resolution *in situ* atmospheric turbulent fluxes in the MABL and simultaneously documented the characteristics of the surface wave field with various remote sensors. The LongEZ (registration N3R) research aircraft (Fig. 1) has proven to be an especially powerful tool for studying the spatial variability of air-sea interaction (e.g., Crawford et al. 1993a; Mourad 1999; Vogel and Crawford 1999; Vogel et al. 1999; Mourad et al. 2000; Mahrt et al. 2001; Sun et al. 2001; Vandemark et al. 2001; Vickers et al. 2001). More information about the airplane and its suite of sensors is provided by Crawford et al. (2001) and Crescenti et al. (2002).

**Fig. 1.** LongEZ N3R in flight.

A case study has been selected to briefly examine the 10-m neutral drag coefficient $C_{DN}$ as a function of various turbulence and sea state parameters over a repeated flight track.

## 2. DATA

The CBLAST-Low pilot study was conducted during a three-week period in July and August 2001 off the south shore of Martha's Vineyard Island, Massachusetts. A total of twenty missions (~ 48 flight hours) were flown by N3R on days with light winds (< 9 m $s^{-1}$) under various atmospheric stabilities. Numerous flux legs and MABL profiles were acquired during the course of the study. When possible, N3R flew over other CBLAST-Low "assets",

*Corresponding author address:* Dr. Tamara K. Grimmett, NRC Postdoctoral Associate, U.S. Dept. Commerce / NOAA, Air Resources Laboratory, 1750 Foote Drive, Idaho Falls, ID 83402; e-mail: tami@noaa.inel.gov

including the R/V *Asterias*, the Air-Sea Interaction Meteorology (ASIMET) buoy (40° 59.5' N, 70° 35.9' W), a three-dimensional sea surface temperature array (41° 15.0' N, 70° 36.0' W), and the Martha's Vineyard Coastal Observatory (MVCO) meteorology tower (41° 59.5' N, 70° 35.9' W). This case study examines data acquired by N3R on Flight 01 conducted on 21 July 2001 between 0900 and 1230 EDT. A total of twelve north-south flux legs at 10-m above the ocean surface were flown by N3R near the southern coast of Martha's Vineyard out to 35 to 40 km (Fig. 2).

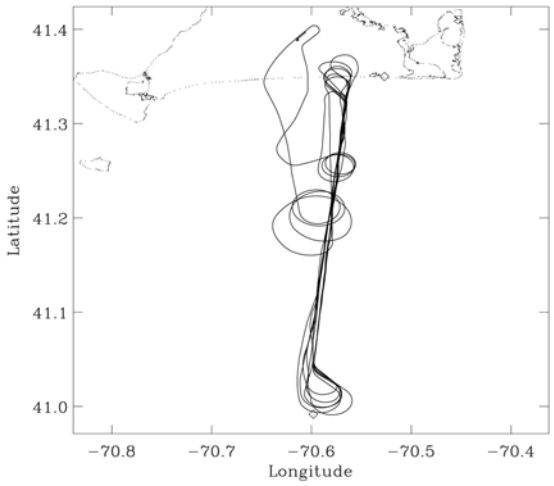


**Fig. 2.** N3R track for Flight 01 on 21 July 2001.

*In situ* data acquired by N3R included horizontal and vertical wind velocity, air temperature, humidity, and pressure. These data were acquired at a rate of 50 Hz. Upward looking and downward looking infrared radiometers measured sky and sea surface temperature (SST), respectively. Other remote sensors included an array of downward looking laser altimeters to measure the vector normal to the sea surface plane (i.e., wave slope of intermediate scale waves on the order of 1 to 10 m). Other derived products include significant wave height, dominant wavelength of the wind sea, and the slope variance of the measured 2D probability density function (i.e., mean square slope or slope variance). Along-track changes in the integrated roughness of short ocean waves on the order of 2 to 100 cm are determined using a 36-GHz continuous wave scatterometer (Vandemark et al. 2001). More specific information on the various sensors and acquired data are given by Crescenti et al. (2001).

## 3. ANALYSIS

Fair weather dominated the CBLAST-Low study sight on 21 July 2001. A large high pressure system was centered over Virginia and extended from the mid-Atlantic states up throughout New England. Humidity was generally low under clear skies. Winds were initially calm in the early morning hours in Martha's Vineyard becoming southwesterly at about 4 m $s^{-1}$ by late morning to early afternoon.

### 3.1 *MABL Structure*

The vertical structure of the MABL over the study sight was documented by N3R (Fig. 3). The potential temperature profile depicts stable conditions from near the surface (~15 m) up to 300 m with a temperature increase of 5 K over that depth. From 300 m to just under 800 m, the MABL is fairly well mixed. The MABL is capped by a strong inversion with the free atmosphere above 900 m. The specific humidity quickly decreases from 10 to about 6 g $kg^{-1}$ from near the surface up to 50 m. Between 50 and 800 m, the specific humidity is generally constant with values between 6 and 7 g $kg^{-1}$. Extremely dry conditions are observed above 800 m, indicative of the free atmosphere. The wind speed is generally light (2 to 4 m $s^{-1}$) from the surface up to 800 m. The wind speed quickly increases to about 5 to 6 m $s^{-1}$ above 800 m. In general, the wind direction veers with height in the MABL. At the surface, the winds are from the south. The wind direction veers in a near-linear fashion from southerly to westerly from the surface to 200 m. Between 200 and 500 m, the winds are from the west-southwest. They continue to veer with height above 500 and become northerly above 600 m. The vertical velocity profile shows regions of increased turbulence near the surface and in the layer between 600 and 800 m.

### 3.2 *Turbulent Fluxes*

Turbulent fluxes and parameters were calculated using standard eddy correlation techniques (e.g., Stull 1988). These values were computed in 60-s blocks which correspond to approximately 3 km in space. These flux measurements were linearly detrended and corrected for aircraft speed variation (Crawford et al. 1993b).

The sensible and latent heat fluxes are defined as

$$H_S = \rho C_p \overline{w'\theta'} \qquad (1)$$

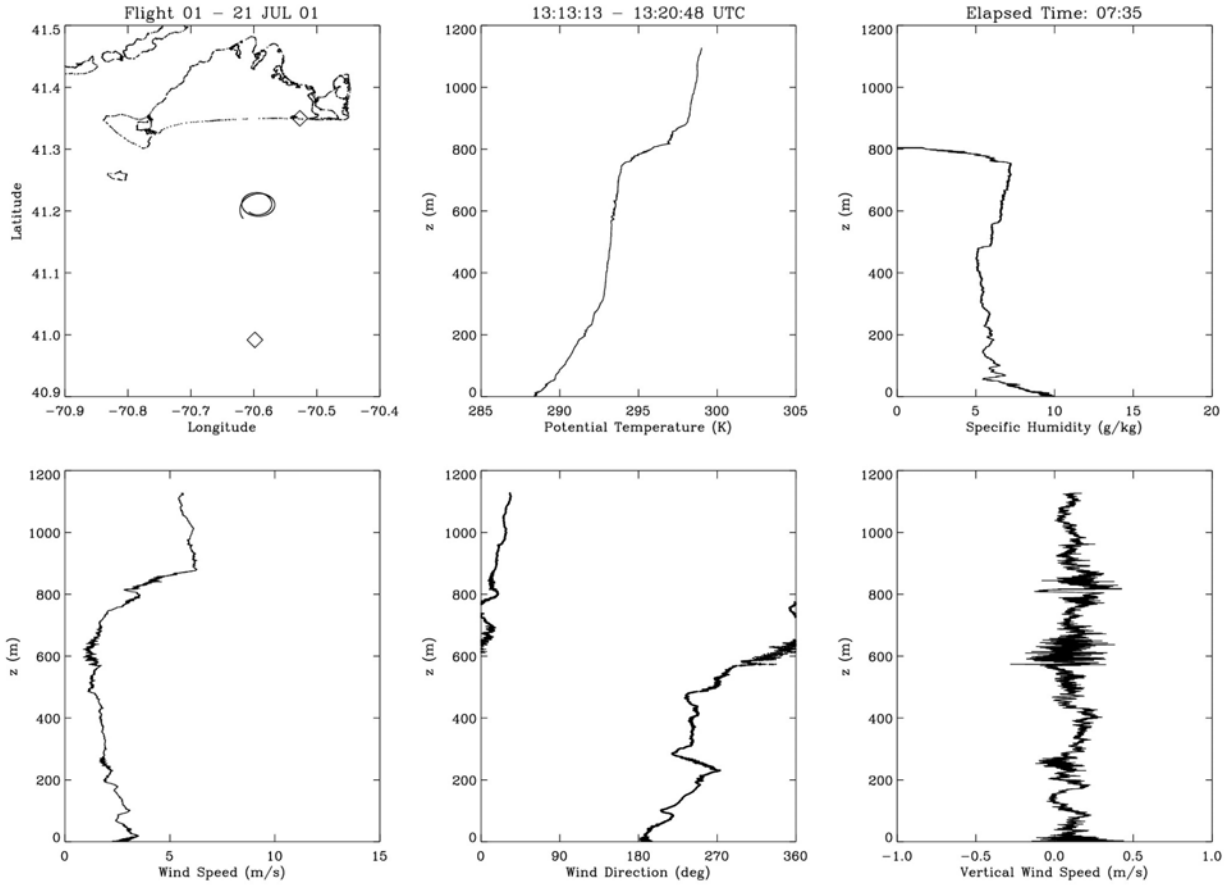


**Fig. 3.** MABL profiles of potential temperature, specific humidity, wind speed, wind direction, and vertical wind velocity from Flight 01 on 21 July 2001.

$$H_E = \rho L_V \overline{w'q'} \qquad (2)$$

where $\rho$ is the dry air density, $C_P$ is the specific heat at constant pressure, Lv is the latent heat of vaporization, and w', $\theta$', and q' are the vertical wind velocity, potential temperature, and specific humidity perturbations, respectively. The wind stress (momentum flux) is defined as

$$\tau = \left[ \left(-\rho \overline{u'w'}\right)^2 + \left(-\rho \overline{v'w'}\right)^2 \right]^{1/2} \qquad (3)$$

where u' and v' are the eastward and northward wind velocity perturbations, respectively. The friction velocity is simply defined as

$$u_* = \left(\frac{\tau}{\rho}\right)^{1/2} \qquad (4)$$

The drag coefficient is defined as

$$C_D = \frac{u_*^2}{U_{10}^2} \qquad (5)$$

where $U_{10}$ is the 10-m wind speed.

Atmospheric stability is estimated as z/L, where z is the altitude of measurement and L is the Monin-Obukhov length defined as

$$L = \frac{-u_*^3 \Theta_V}{k g \overline{w'\Theta_V'}} \qquad (6)$$

where $\theta_V$ is the virtual potential temperature, k is the von Karman constant (0.4), and g is the acceleration due to gravity (9.81 m $s^{-2}$). Various mean and turbulence parameters are shown in Fig. 4 along the length of the flight track.

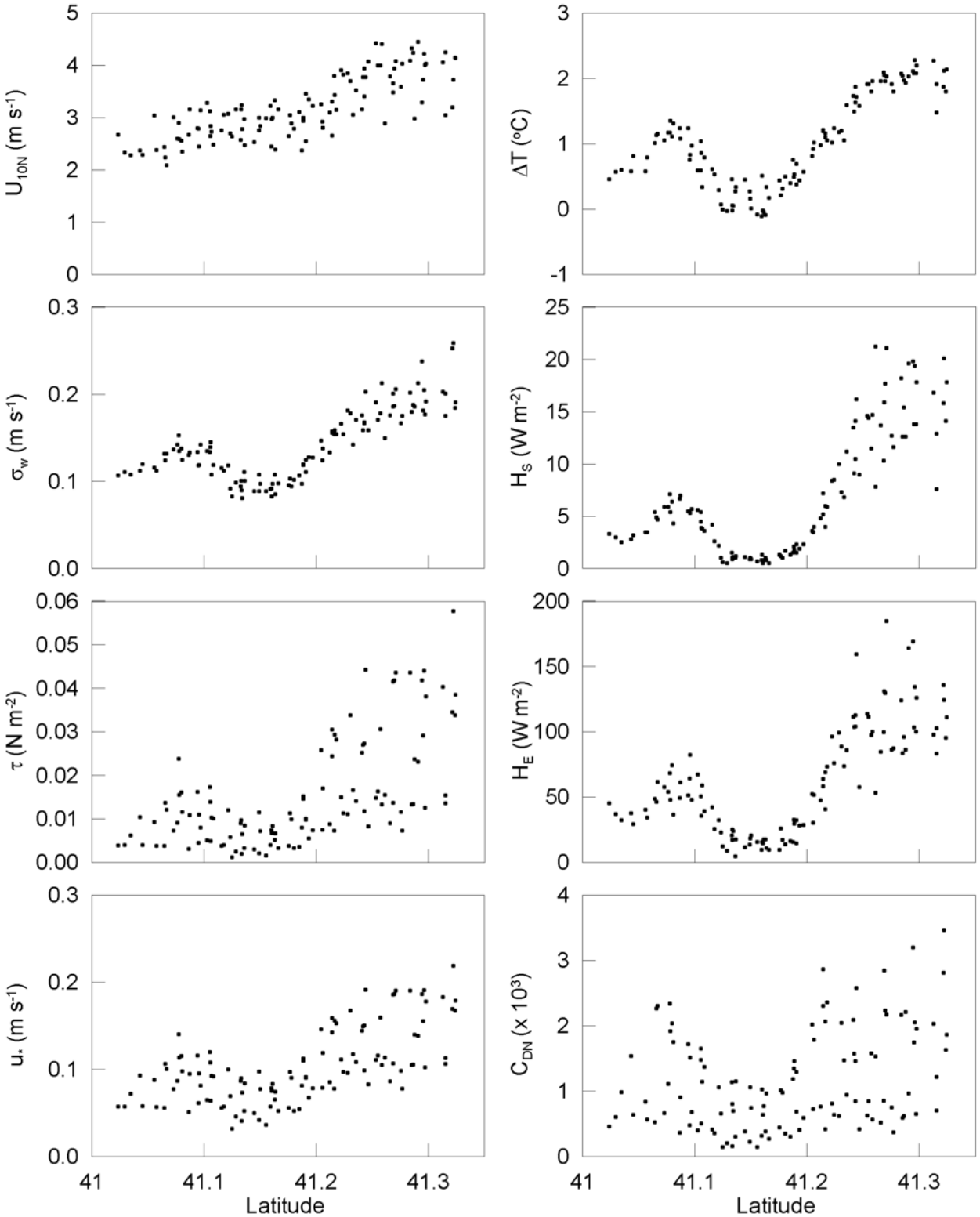


**Fig. 4.** Flight 01 turbulence parameters. Left column: 10-m neutral wind speed ($U_{10N}$), standard deviation of the vertical wind speed ($\sigma_w$), wind stress ($\tau$), and friction velocity ($u_*$). Right column: air-sea temperature difference ($\Delta T$), sensible heat flux ($H_S$), latent heat flux ($H_E$), and 10-m neutral drag coefficient ($C_{DN}$).

These parameters include the 10-m neutral mean wind speed ($U_{10N}$), air-sea temperature difference ($\Delta T$ = SST - T), where T is the air temperature, standard deviation of the vertical wind speed ($\sigma_w$), wind stress ($\tau$), friction velocity ($u_*$), 10-m neutral drag coefficient ($C_{DN}$), and sensible heat flux ($H_S$) and latent ($H_E$) heat flux.

Winds were about 2 m $s^{-1}$ from the south-southwest at the southern end of the flux legs and increased linearly to about 4.5 m $s^{-1}$ from the southwest near the coastline.

The air-sea temperature difference $\Delta T$ increases from 0.5 to 1.5 °C over the first 5 km at the southern end of the flux legs with a local maxima about 25 km from the shoreline. Note a positive $\Delta T$ represents colder air over warmer water, i.e., an unstable atmospheric boundary layer. Over the next 8 km, $\Delta T$ decreases to about 0 °C, representing a local minima about 17 km from the shoreline. $\Delta T$ increases from 0 °C to slightly over 2 °C from 17 km to the coastline.

Stability estimates (z/L) averaged -1.1 with a standard deviation of 1.0, indicating an unstable MABL, at least at the flight level of 10 m. No values of z/L where greater than 0. Yet the MABL profiles show a stable MABL from near the surface up to 300 m. It appears that the convective instability is limited to the first 10 to 20 m above the ocean surface.

Most of the turbulence parameters shown in Fig. 4 display high correlations to $\Delta T$. The fluxes of sensible and latent heat ($H_S$ and $H_E$) are highly correlated (r = 0.94 and 0.88) to $\Delta T$. As expected for a MABL, the latent heat flux is an order of magnitude larger than the sensible heat flux. Note that as $\Delta T$ approaches 0 °C, so do the sensible and latent heat fluxes.

Vertical mixing $\sigma_w$ is highly correlated to $\Delta T$ (r = 0.92). The wind stress $\tau$ and friction velocity $u_*$ are also well correlated to $\Delta T$ (r = 0.70 and 0.73, respectively) but show considerably more scatter near the shoreline. This is probably due to shoaling of waves in shallower waters. The 10-m neutral drag coefficient $C_{DN}$ shows considerable scatter both at the southern and northern ends of the flux legs were the boundary layer is unstable ($\Delta T$ > 0 °C). Conversely, much less scatter is observed over the waters where $\Delta T$ approaches 0 °C. Clearly under these light wind conditions, these turbulent fluxes are driven by the air-sea temperature gradient.

### 3.3 *Sea State*

The normalized radar cross section (NRCS) is a measure of surface roughness (Vandemark et al. 2001). NRCS is determined from the nadir-looking Ka-band scatterometer. This instrument is used to determine short-wave characteristics of the sea surface. For a nadir-looking scatterometer the return power is greatest from a smooth sea surface. As the sea surface roughens, the scatterometer signal is scattered and the return is decreased. Thus, NRCS is largest for smooth surfaces and decreases as the surface roughens.

The significant wave height (SWH) is another measure of the sea state and is defined as four times the standard deviation of the wave height. The wave height is calculated as the difference between the known altitude of the aircraft and the averaged laser altimeter measurement, both corrected to earth-based coordinates.

Fig. 5 shows estimates of the NRCS and the SWH for the twelve flux legs of Flight 01. The NRCS ranges between 14 and 16 dB at the southern end of the flux legs and decreases slightly moving north. After reaching a small minimum, the NRCS quickly increases to a maximum value of 17 dB about 17 km from the shoreline. It is at this location where the ocean surface is smoothest. It also coincides with the location where $\Delta T$ = 0 °C and the fluxes of heat, moisture, and momentum are at a minimum. NRCS decreases from that point to the shoreline, indicating an increase of sea surface roughness. Note that the mean wind speed increased in magnitude closer to shore. Thus, the rougher sea state is attributed to small-scale wind-generated waves.

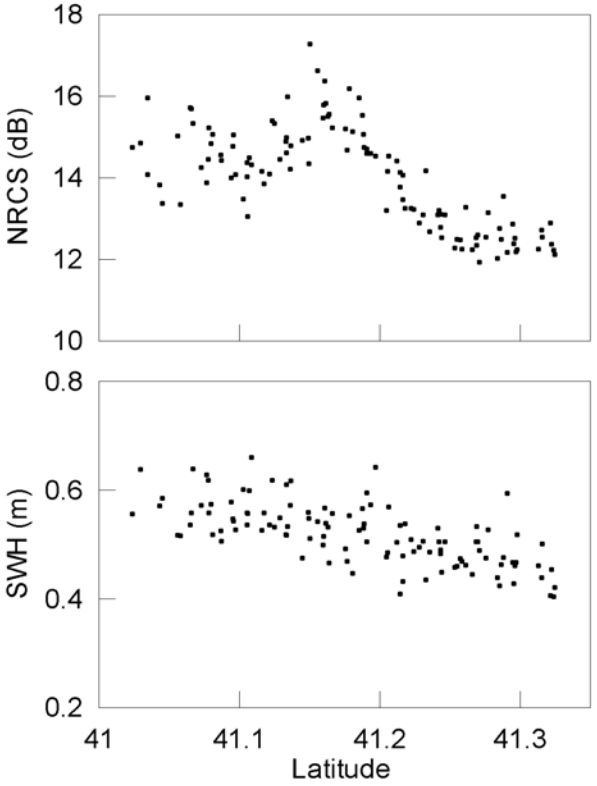


**Fig. 5.** NRCS and SWH for Flight 01.

The SWH decreases linearly from 0.6 to 0.4 m from the southern to northern ends of the flux legs, respectively. The larger wave heights at the southern end of the flux legs are probably due to long-wave ocean swell which decrease in height as the shoreline is approached. There is no obvious dependence of SWH with any of the various turbulent fluxes or parameters.

The dependence of NRCS as a function of sensible and latent heat flux and turbulent kinetic energy is shown in Fig. 6. As the sensible and latent heat fluxes increase, so does the roughness of the sea surface (decrease in NRCS). Turbulent convection contributes to the formation of small-scale wind-generated waves. This is further supported by the plot showing the strong dependence of surface roughness with turbulent kinetic energy and indicates the increase in turbulent velocity fluctuations. These results should be expected for conditions where turbulent heating and mixing are dominant.

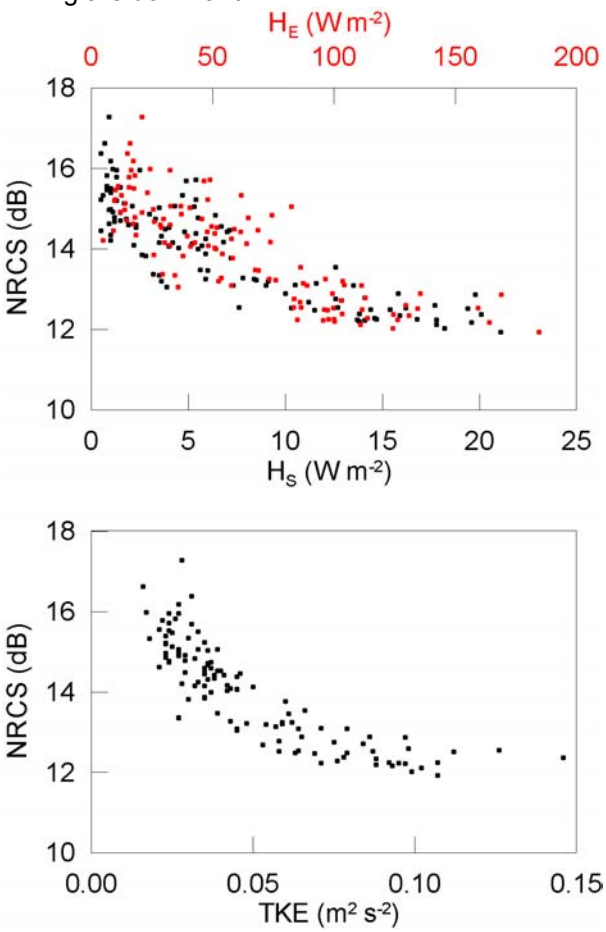


**Fig. 6.** NRCS as a function of (top) sensible and latent heat fluxes and (bottom) turbulent kinetic energy.

3.4 *Drag Coefficient*

The 10-m neutral drag coefficient $C_{DN}$ is shown as a function of various mean and turbulent flux values in Fig. 7. $C_{DN}$ shows considerable scatter as a function of the 10-m neutral wind speed $U_{10N}$. Of course, most of the values for $U_{10N}$ vary between 2 and 4 m s$^{-1}$. On the other hand, $C_{DN}$ exhibits a dependence on $\sigma_w$. $C_{DN}$ displays good agreement with $\tau$, which is due to self-correlation of those values which are used to derive $C_{DN}$. The drag coefficient is compared to the absolute difference between the mean wind direction $\theta_U$ and the wind stress direction $\theta_t$. For small differences, the scatter in $C_{DN}$ is considerable. However, for large differences between the vectors, the drag coefficient is rather small. The high $C_{DN}$ value at about 80° on the abscissa is being investigated.

The drag coefficient displays a dependence on air-sea temperature difference $\Delta T$. The sensible and latent heat fluxes show similar behavior, however, with considerably more scatter. Small values of $C_{DN}$ are found for very unstable values of z/L while considerable scatter in $C_{DN}$ is seen for z/L values approaching zero.

The distribution of $C_{DN}$ as a function of the turbulent kinetic energy is similar to that of $\Delta T$. However, a clear dependence of drag coefficient to the turbulent intensity (turbulent kinetic energy divided by the mean kinetic energy) with a correlation coefficient of 0.84. $C_{DN}$ displays an inverse relationship with NRCS. However, no definite conclusions can be made due to the considerable scatter seen in this particular case. $C_{DN}$ is also compared to the roughness Reynolds number $R_r$ which is define as

$$R_r = \frac{z_o u_*}{\nu} \qquad (7)$$

where $\nu$ is viscosity of air and $z_o$ is the roughness length which is estimated from the simple relation

$$z_o = \frac{\alpha u_*^2}{g} \qquad (8)$$

where $\alpha$ is the Charnock constant (0.011). There is a strong linear dependence of $C_{DN}$ on $R_r$ for values of $R_r < 0.2$, however, considerable scatter is seen for values of $R_r > 0.2$.

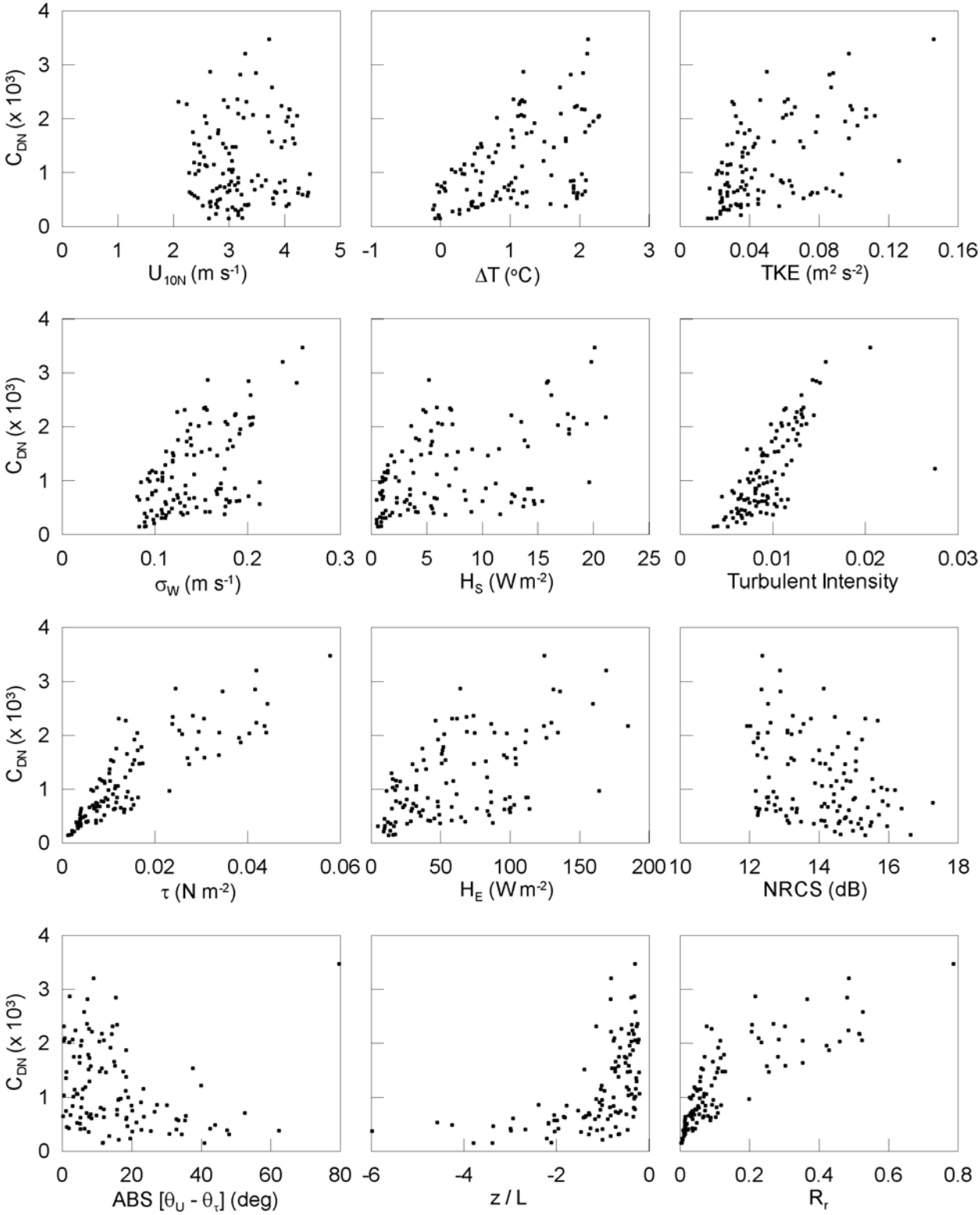


**Fig. 7.** 10-m neutral drag coefficient as a function of (left column) 10-m neutral wind speed ($U_{10N}$), standard deviation of the vertical wind speed ($\sigma_w$), wind stress ($\tau$), absolute difference between the mean wind direction and stress direction ($\theta_U - \theta_\tau$), (center column) air-sea temperature difference ($\Delta T$), sensible ($H_S$) and latent ($H_E$) heat flux, stability (z/L), (right column) turbulent kinetic energy (TKE), turbulent intensity, NRCS, and roughness Reynolds number ($R_r$).

## 4. DISCUSSION

An experiment similar to this one was conducted by Plant et al. (1999) using a blimp over the Pacific Ocean. They measured many of the same quantities for days with neutral to stable conditions. Under these conditions, they saw no $\Delta T$ forcing. Also, they did not see much scatter in $u_*$ except at higher wind speeds (9-10 m $s^{-1}$) unlike the data shown in Fig. 4. Our data exhibits quite a bit of scatter in $u_*$, more so than in the latent and sensible heat fluxes except as land is approached. This could be due to the increase in wind speed closer to land. For their conditions, Plant et al. (1999) identified a threshold wind speed of the ocean of 2 m $s^{-1}$ above which momentum transfer is supported by surface roughness elements. Below this wind speed, viscous effects dominate which dampen the growth of short waves. Therefore, the short waves do not act as roughness elements to increase $u_*$ and momentum transfer ends up supported by viscous effects. A value of $u_*$ = 0.1 m $s^{-1}$ corresponded to the 2 m $s^{-1}$ wind speed for the Plant et al. (1999) data. But this was arrived at from a more statistically significant sample than is represented in Fig. 4. Unfortunately our wind speeds do not go below 2 m $s^{-1}$ but further investigation of the $u_*$ values below 0.1 m $s^{-1}$ is required.

Near land, the increase in $u_*$ (Fig. 4) and the decrease in NRCS (Fig. 5) are not contradictory. As the waves break, the surface roughness is increased and the average height of the waves decreases. Thus NRCS decreases (surface roughness increases) and SWH decreases.

## 5. SUMMARY

Data were acquired by the LongEZ N3R research aircraft during a three-week period in summer 2001 during the CBLAST-Low pilot field study over the ocean south of Martha's Vineyard. These data are to be used in the examination of air-sea interaction under light wind conditions. A case study was selected in which N3R flew twelve repeated north-south flux legs at 10 m altitude from the coastline out to about 40 km. The mean structure of the MABL displays stable conditions from 20 m up to about 300 m while the lowest 10 m show moderate instability with upward fluxes of heat, moisture, and momentum. Southerly to southwesterly winds were generally light with values between 2-4 m $s^{-1}$. Many of the turbulent fluxes show a clear dependence on the air-sea temperature difference. The turbulent fluxes of heat, moisture, and momentum also have a direct impact on the surface roughness of the ocean by increasing turbulent velocity fluctuations. The 10-m neutral drag coefficient, on the other hand, does not show a clear correlation with many of these turbulence parameters displaying considerable scatter in most instances. Analysis of this data is onging.

## 6. ACKNOWLEDGMENTS

This work was supported by the Office of Naval Research under contract N00014-01-F-0008. The authors would like to express their thanks to Jeff French for his efforts in providing a high quality data set. This work was performed while TKG held a National Research Council Research Award at NOAA's Air Resources Laboratory Field Research Division in Idaho Falls, Idaho.

## 7. REFERENCES

Crawford, T. L., R. T. McMillen, T. P. Meyers, and B. B. Hicks, 1993a: Spatial and temporal variability of heat, water vapor, carbon dioxide, and momentum air-sea exchange in a coastal environment. *J. Geophys. Res.*, **98**, 12869-12880.

Crawford, T. L., R. T. McMillen, R. J. Dobosy, and I. MacPherson, 1993b: Correcting airborne flux measurements for aircraft speed variation. *Bound.-Layer Meteor.*, **66**, 237-245.

Crawford, T. L., G. H. Crescenti, and J. M. Hacker, 2001: Small environmental research aircraft (SERA): the future of airborne geoscience. *Eleventh Symposium on Meteorological Observations and Instrumentation*, Albuquerque, NM, Amer. Meteor. Soc., 117-122.

Crescenti, G. H., J. R. French, and T. L. Crawford, 2001: Aircraft measurements in the Coupled Boundary Layers Air-Sea Transfer (CBLAST) light wind pilot field study. NOAA Tech. Memo. OAR ARL-241, Silver Spring, MD, 82 pp.

Crescenti, G. H., J. R. French, T. L. Crawford, and D. C. Vandemark, 2002: An integrated airborne measurement system for the determination of atmospheric turbulence and ocean surface wave field properties. *Sixth Symposium on Integrated Observing Systems*, Orlando, FL, Amer. Meteor. Soc., 60-67.

Drennan, W. M., K. K. Kahma, and M. A. Donelan, 1999: On momentum flux and velocity spectra over waves. *Bound.-Layer Meteor.*, **92**, 489-515.

Greischar, L. and R. Stull, 1999: Convective transport theory for surface fluxes tested over the western Pacific warm pool. *J. Atmos. Sci.*, **56**, 2201-2211.

Lambert, D., and P. Durand, 1999: The marine

atmospheric boundary layer during SEMAPHORE. Part I: Mean vertical structure and non-axisymmetry of turbulence. *Quart. J. Roy. Meteor. Soc.*, **125**, 495-512.

Mahrt, L., D. Vickers, J. Howell, J. Hojstrup, J. Wilczak, J. Edson, and J. Hare, 1996: Sea surface drag coefficients in RASEX. *J. Geophys. Res.*, **101**, 14327-14335.

Mahrt, L., D. Vickers, J. Sun, T. L. Crawford, G. Crescenti, and P. Frederickson, 2001: Surface stress in offshore flow and quasi-frictional decoupling. *J. Geophys. Res.*, **106**, 20629-20639.

Mourad, P. D., 1999: Footprints of atmospheric phenomena in synthetic aperture radar images of the ocean surface: a review. *Air-Sea Exchange: Physics, Chemistry and Dynamics*, G. L. Geernaert, Ed., Kluwer Academic Publishers, 269-290.

Mourad, P. D., D. R. Thompson, and D. C. Vandemark, 2000: Extracting fine-scale wind fields from synthetic aperture radar images of the ocean surface. *John Hopkins APL Tech. Digest*, **21**, 108-115.

Plant, W. J., D. E. Weissman, W. C. Keller, V. Hessany, K. Hayes, and K. W. Hoppel, 1999: Air/Sea momentum transfer and the microwave cross section of the sea. *J. Geophys. Res.*, **104**, 11173-11191.

Ramage, C. S., 1984: Can shipboard measurements reveal secular changes in tropical air-sea heat flux? *J. Climate Appl. Meteor.*, **23**, 187-193.

Serra, Y. L., D. P. Rogers, D. E. Hagan, C. A. Friehe, R. L. Grossman, R. A. Weller, and S. Anderson, 1997: Atmospheric boundary layer over the central and western equatorial Pacific Ocean observed during COARE and CEPEX. *J. Geophys. Res.*,**102**, 23217-23237.

Stull, R. B., 1988: *An Introduction to Boundary Layer Meteorology*. Kluwer Academic Publishers, 666 pp.

Sun, J., J. F. Howell, S. K. Esbensen, L. Mahrt, C. M. Greb, R. Grossman, and M. A. LeMone, 1996: Scale dependence of air-sea fluxes over the western equatorial Pacific. *J. Atmos. Sci.*, **53**, 2997-3012.

Sun, J., D. Vandemark, L. Mahrt, D. Vickers, T. Crawford, and C. Vogel, 2001: Momentum transfer over the coastal zone. *J. Geophys. Res.*, **106**, 12437-12448

Vandemark, D., P. D. Mourad, S. A. Bailey, T. L. Crawford, C. A. Vogel, J. Sun, and B. Chapron, 2001: Measured changes in ocean surface roughness due to atmospheric boundary layer rolls. *J. Geophys. Res.*, **106**, 4639-4654.

Vickers, D., L. Mahrt, J. Sun, and T. Crawford, 2001: Structure of offshore flow. *Mon. Wea. Rev.*, **129**, 1251-1258.

Vogel, C. A., and T. L. Crawford, 1999: Exchange measurements above the air-sea interface using an aircraft. *Air-Sea Exchange: Physics, Chemistry and Dynamics*, G. L. Geernaert, Ed., Kluwer Academic Publishers, 231-245.

Vogel, C. A., T. L. Crawford, J. Sun, and L. Mahrt, 1999: Spatial variation of the atmospheric surface drag coefficient within a coastal shoaling zone. *13th Symposium on Boundary Layers and Turbulence*, Dallas, TX, Amer. Meteor. Soc., 347-348.